

Long Duration X-Ray Flash and X-Ray Rich Gamma Ray Burst from Low Mass Population III Star

Daisuke Nakauchi¹, Yudai Suwa², Takanori Sakamoto^{3,4,5}, Kazumi Kashiyama^{1,6}, and
Takashi Nakamura¹

¹*Department of Physics, Kyoto University, Oiwake-cho, Kitashirakawa, Sakyo-ku, Kyoto
606-8502, Japan*

²*Yukawa Institute for Theoretical Physics, Kyoto University, Oiwake-cho, Kitashirakawa,
Sakyo-ku, Kyoto 606-8502, Japan*

³*Center for Research and Exploration in Space Science and Technology (CRESST), NASA
Goddard Space Flight Center, Greenbelt, MD 20771*

⁴*Joint Center for Astrophysics, University of Maryland, Baltimore County, 1000 Hilltop
Circle, Baltimore, MD 21250*

⁵*NASA Goddard Space Flight Center, Greenbelt, MD 20771*

⁶*Department of Astronomy and Astrophysics, Pennsylvania State University, University
Park, PA 16802, USA*

ABSTRACT

Recent numerical simulations suggest that Population III (Pop III) stars were born with masses not larger than $\sim 100M_{\odot}$ but typically $\sim 40M_{\odot}$. By self-consistently considering the jet generation and propagation in the envelope of these low mass Pop III stars, we find that a Pop III blue super giant star has the possibility to raise a gamma-ray burst (GRB) even though it keeps a massive hydrogen envelope. We evaluate observational characters of Pop III GRBs and predict that Pop III GRBs have the duration of $\sim 10^5$ sec in the observer frame and the peak luminosity of $\sim 5 \times 10^{50}$ erg sec⁻¹. Assuming that the $E_p - L_p$ (or $E_p - E_{\gamma,\text{iso}}$) correlation holds for Pop III GRBs, we find that the spectrum peak energy falls \sim a few keV (or ~ 100 keV) in the observer frame. We discuss the detectability of Pop III GRBs by future satellite missions such as *EXIST* and *Lobster*. If the $E_p - E_{\gamma,\text{iso}}$ correlation holds, we have the possibility to detect Pop III GRBs at $z \sim 9$ as long duration X-ray rich GRBs by *EXIST*. On the other hand, if the $E_p - L_p$ correlation holds, we have the possibility to detect Pop III GRBs up to $z \sim 19$ as long duration X-ray flashes by *Lobster*.

Subject headings: gamma rays: bursts — gamma rays: observations — gamma rays: theory

1. Introduction

Gamma ray bursts (GRB) are the brightest phenomena in the universe. Long-soft type GRBs are considered to originate from deaths of massive stars such as Wolf-Rayet (WR) stars (Hjorth & Bloom 2011). The most widely accepted scenario for long GRBs is the collapsar scenario (Woosley 1993; MacFadyen & Woosley 1999). In this model, after the gravitational collapse of a massive stellar core, a black hole and an accretion disk system is formed and it launches a relativistic jet by magnetic field or neutrino pair annihilation process. If the jet can break out the stellar envelope successfully, a GRB is raised by converting the jet kinetic energy into the radiation energy.

Owing to their brightness and detections at high redshift universe, GRBs are expected to be one of the powerful tools to probe the early universe. The development of observational instruments and early follow-up systems enable us to discover some high redshift GRBs. The most distant one ever is GRB 090429B at $z = 9.4$ (Cucchiara et al. 2011) and GRB 090423 at $z = 8.3$ (e.g. Tanvir et al. 2009; Salvaterra et al. 2009; Chandra et al. 2010) follows it. If GRBs can be raised by first stars and detected, we will draw informations about the early universe, e.g., the star formation history and the reionization history.

First stars in the universe, so called Population III (Pop III) stars, are considered to be formed from metal free gas in the very early universe. The metal-free primordial gas cools less efficiently compared to the metal-contained present-day gas, which allows the primordial gas to have larger fragmentation masses. Since it was considered that the whole fragmented gas clump collapsed to form a single star, Pop III stars were theoretically predicted to be very massive $\sim 100 - 1000 M_{\odot}$ (Abel et al. 2002; Bromm et al. 2002). However, recent studies suggest that this is not always the case and that a massive gas clump can experience further fragmentation to form a binary system (Turk et al. 2009; Stacy et al. 2010; Clark et al. 2011). Tan & McKee (2004) and McKee & Tan (2008) suggested that the UV radiation from the central protostar can ionize the surrounding neutral gas and suppress the accretion onto the protostar. They analytically investigated this feed back effect on the protostar evolution and found that Pop III stars finally obtain mass typically $\sim 140 M_{\odot}$. More recently, Hosokawa et al. (2011) performed two-dimensional simulations of the protostar evolution including the above feed back effect and found that Pop III stars finally obtain masses typically $\sim 40 M_{\odot}$. They also concluded that the UV radiation from the central star eventually stops the mass accretion and the growth of the star by the evaporation of the surrounding gas.

It is considered that metal free Pop III stars do not lose mass, keeping large hydrogen envelopes until the pre-supernova stage, because of the low opacity envelopes (Woosley et al. 2002). The final fate of a Pop III star depends on the stellar mass (Heger et al. 2003). After

the stellar core collapse, those Pop III stars in the range of $10M_{\odot} \lesssim M \lesssim 25M_{\odot}$ would explode as supernovae and form neutron stars as remnants. Those in $25M_{\odot} \lesssim M \lesssim 40M_{\odot}$ form black holes as remnants after the fall back accretion of the envelopes onto the temporally formed neutron stars. More massive stars ($40M_{\odot} \lesssim M \lesssim 140M_{\odot}$ and $260M_{\odot} \lesssim M$) would fail to blow out their envelopes and promptly form massive black holes, except those stars in $140M_{\odot} \lesssim M \lesssim 260M_{\odot}$ who end as pair-instability supernovae due to the explosive nucleosynthesis. These remnant massive black holes are expected to raise various violent phenomena (Fryer et al. 2001; Suwa et al. 2007).

There have been some studies about the productivity of GRBs from massive Pop III stars ($\gtrsim 100M_{\odot}$) (Mészáros & Rees 2010; Komissarov & Barkov 2010; Suwa & Ioka 2011; Nagakura et al. 2012). The former two studies assumed a massive black hole surrounded by an accretion disk as an outcome of a massive stellar collapse, and estimated the accretion rate onto the black hole. Then they evaluated the jet luminosity and showed that the burst activity of a Pop III star is observable by current detectors. In Suwa & Ioka (2011), they analytically studied the jet propagation in the stellar envelope and showed that massive Pop III stars ($\sim 900M_{\odot}$) can produce GRBs although they have large hydrogen envelopes, since the long lasting accretion provides enough energy and time for the successful jet breakout. In addition, Nagakura et al. (2012) performed two-dimensional relativistic hydrodynamic simulations in which the accretion onto a black hole and the jet production are treated in a self-consistent way for stellar models of massive Pop III stars ($915M_{\odot}$), Wolf-Rayet stars (initially $16M_{\odot}$), and low mass Pop III stars ($40M_{\odot}$). They confirmed the validity of the analytic results in Suwa & Ioka (2011) and also found that $40M_{\odot}$ Pop III stars can be progenitors of GRBs, but did not study their observational characteristics and detectability.

The idea of GRBs from blue super giants (BSG) was suggested in Mészáros & Rees (2001). Although they considered the jet dynamics in the stellar envelope, they treated a steady jet and did not reflect the central engine activity caused by the change of the accretion rate. They did not evaluate the possibility of GRBs from BSGs quantitatively. On the other hand, Woosley & Heger (2012) discussed gamma-ray transients from Pop III BSG collapsars by investigating the mass accretion of the outermost layers of a star, but did not discuss the jet propagation and the jet break out. Assuming that the conversion efficiency of the accretion energy to the radiation energy $\sim 10^{-2}$, they found that Pop III BSGs can produce long gamma-ray transients with duration 10^{4-5} sec and luminosity 10^{48-49} erg sec $^{-1}$. In this paper, we simultaneously investigate both aspects (the jet propagation and the central engine activity) in a self-consistent way by including the following physical processes; the stellar collapse, the non-steady jet injection, and the jet propagation in the stellar envelope. By doing this, we quantitatively discuss the possibility of the jet break out and GRB especially for low mass Pop III stars (around $40M_{\odot}$).

In §2, after introducing the stellar models and the jet propagation models, we investigate the productivity of a GRB focusing on a $40M_{\odot}$ Pop III star, which is a Pop III star with the typical mass reported by the state-of-the-art simulation done in Hosokawa et al. (2011). In §3, we calculate the observational characters, such as the duration T_{90} , the peak luminosity L_p and the spectrum peak energy in the observer frame E_p^{obs} , of GRBs from $40M_{\odot}$ Pop III progenitors. Then we evaluate the detectability of such Pop III GRBs by future detectors such as *Lobster* and *EXIST* in detail, varying the redshift of a burst. We apply the above discussions to different progenitor models with masses of $30 - 90M_{\odot}$. In the last part of §3, we evaluate the light curves of Pop III GRB radio afterglow emissions and their detectability by the Low Frequency Array (LOFAR) and the Expanded Very Large Array (EVLA). §4 is devoted to the summary and discussions.

2. GRBs from low mass Pop III stars

2.1. Progenitor and Relativistic Jet models

We employ a pre-collapse stellar model of z40.0 by Woosley et al. (2002), which provides the structure of a $40M_{\odot}$ with zero metallicity at the final phase of the stellar evolution. It is considered that a $40M_{\odot}$ Pop III star promptly forms a black hole after the core collapse (Heger et al. 2003). Then we consider the subsequent evolution of the stellar collapse and the jet propagation in the stellar envelope following the similar prescription to Suwa & Ioka (2011).

We first assume that the collapse proceeds in a spherically symmetric manner without pressure support so that each mass shell of the star within mass $[M_r, M_r + dM_r]$ and radius $[r, r + dr]$ falls into the central core in the free-fall time scale $t_{\text{ff}}(r) = \sqrt{r^3/GM_r}$. We calculate the mass accretion rate from the expression $\dot{M}(r) = dM_r/dt_{\text{ff}}(r)$. When the mass of the central core becomes $3M_{\odot}$, we identify that a black hole is formed since the maximum possible mass of a neutron star is $\sim 3M_{\odot}$ (Rhoades & Ruffini 1974; Chitre & Hartle 1976). After the formation of the black hole, we assume that a cold relativistic jet with a constant opening angle $\theta_j = 5^\circ$ has been launched and we take this moment as the origin of time ($t = 0$).

There are mainly two candidates for the jet production mechanisms, i.e., the neutrino annihilation process and the magnetic process. In Suwa & Ioka (2011), they showed that the jet model based on the neutrino annihilation process is not appropriate for producing GRBs from very massive Pop III stars. Accordingly we adopt the jet model based on the magnetic process. In this model, the jet injection luminosity $L_{\text{jet}}(t)$ is considered to be represented as

$L_{\text{jet}}(t) = \eta \dot{M}(t)c^2$ (see Suwa & Ioka 2011 and references there in), where the constant η is an energy conversion efficiency and we take the value of $\eta = 6.2 \times 10^{-4}$. This is a calibrated value so as for Wolf-Rayet stars to reproduce the energetics of canonical local long GRBs, i.e., nearly 10^{52} ergs of energy should be injected into the relativistic jet after the breakout.

In this paper it looks like that we neglect the effect of the stellar rotation and treat the stellar collapse in spherically symmetric way. According to Kumar et al. (2008), when the stellar rotation is taken into consideration, the accretion time scale onto the central BH for each mass shell $t_{\text{acc}}(r)$ can be represented as $t_{\text{acc}}(r) \sim t_{\text{ff}}(r)/\alpha$, where $\alpha \sim 0.1$ is the standard dimensionless viscosity parameter of the disk. As described in Suwa & Ioka (2011), we regard that this uncertain factor is absorbed within the calibrated parameter η . Therefore, we think that the disk formation is implicitly taken into account and that the spherically symmetric prescription makes sense.

In the following sections, we consider the propagation of a jet in the stationary stellar envelope. For the $40M_{\odot}$ Pop III model, the He core mass M_{He} and the He core radius r_{He} are $M_{\text{He}} \sim 22M_{\odot}$ and $r_{\text{He}} \sim 10^{11}$ cm, respectively. Therefore, the collapse time scale of the He core is estimated as $t_{\text{coll}} \sim 600$ sec. On the other hand, the time scale for the jet head to reach the outer edge of the He core can be evaluated as $t_{\text{cross}} \sim r_{\text{He}}/0.1c \sim 30$ sec, since we can see that the average velocity of the jet head within the He core is $\sim 0.1c$ (see Fig. 1). Accordingly, $t_{\text{cross}} \ll t_{\text{coll}}$ holds. We confirm that this inequality holds better in outer layers and that calculations based on the stationary envelope is self consistent.

2.2. Jet Propagation in the Pop III Star Envelope

First, we consider the propagation of a jet in the stellar envelope. As pointed out in the previous subsection, we approximate that the stellar envelope is stationary and that the density profile is the same as that in the pre-supernova stage until the jet break out. A jet propagating through the stellar envelope forms forward and reverse shocks at its head. Here, we assume that the separation between these shocks is small compared to the distance from the stellar center. From the continuity of the momentum flux at the jet head, we have (Matzner 2003),

$$\rho_j c^2 h_j (\Gamma_j \Gamma_h)^2 (\beta_j - \beta_h)^2 + P_j = \rho_* c^2 h_* (\Gamma_h \beta_h)^2 + P_*, \quad (1)$$

where ρ, h, Γ, β and P represent the density, the specific enthalpy, Lorentz factor, the velocity divided by the speed of light c , and the pressure, respectively. The subscripts j, h and * stand for the jet, the jet head and the stellar envelope, respectively. We consider a cold jet so that we can neglect P_j in l.h.s. of Eq. (1). In r.h.s. of Eq. (1), we can approximate

$h_* \sim 1$ and neglect P_* , since stellar material is non-relativistic. Then the velocity of the jet head (β_h) is expressed as

$$\beta_h(t) = \beta_j \left[1 + \left[\frac{\pi r_h^2 \theta_j^2 \rho_*(r_h) c^3}{L_j(t - r_h/(\beta_j c))} \right]^{1/2} \right]^{-1}, \quad (2)$$

where $L_j(t - r_h/(\beta_j c))$ and r_h refer to the jet luminosity and the position of the jet head, respectively. We use the formula $L_j = \pi(r_h \theta_j)^2 \rho_j c^2 h_j \Gamma_j^2 \beta_j c$ in calculating Eq. (2). Accordingly, the position of the jet head is calculated as $r_h(t) = \int_0^t \beta_h(t') c dt'$.

The jet head consists of shocked stellar matter and shocked jet material. They are relativistically hot and expand sideways of the jet forming a cocoon. We assume that almost all the jet energy goes through the shocked region into the cocoon during the jet propagating in the stellar envelope. The cocoon expands laterally by balancing its pressure with the ram pressure of the stellar matter as

$$P_c = \rho_* c^2 h_* \beta_c^2 + P_* \sim \rho_* c^2 \beta_c^2, \quad (3)$$

where the subscript c refers to the cocoon and $P_c \gg P_*$ is assumed. Since the cocoon consists of relativistically hot materials, P_c can be expressed as $P_c = E_c/(3V_c)$, using the cocoon volume V_c and the cocoon energy E_c . Now, we suppose the shape of the cocoon as a cone, then $V_c(t) = \pi r_c^2(t) r_h(t)/3$. In our jet model, the cocoon energy can be expressed as $E_c(t) = \eta M_{\text{acc}}(t) c^2$, where $M_{\text{acc}}(t)$ is the mass accreted to the black hole by the time t . Substituting all these expressions into Eq. (3), the cocoon expansion velocity β_c can be calculated as

$$\beta_c(t) \sim \frac{r_h(t)}{r_c(t)} \sqrt{\frac{4\eta M_{\text{acc}}(t)}{3M(r_h)}}, \quad (4)$$

where $M(r_h) = (4\pi r_h^3/3)\rho_*$. Then the position of the cocoon edge is given as $r_c(t) = \int_0^t \beta_c(t') c dt'$.

Now we discuss whether Pop III stars can raise GRBs by following the time evolution of the positions of the jet head and the cocoon edge. If the jet head reaches the stellar surface earlier than the cocoon edge, we consider that the star can raise a GRB since we can expect a successful jet breakout. On the other hand, if the cocoon edge reaches the stellar surface earlier, we can expect that the mass accretion is suppressed and that the relativistic jet is stalled on the way. This looks like a failed GRB.

Fig. 1 shows the time evolution of the jet head velocity β_h (the red solid line) and the cocoon velocity β_c (the green dashed line). In this figure, the time variability of velocities comes from the discontinuity of the stellar density profile and the mass accretion rate. As

pointed out in e.g., Mészáros & Rees (2001), we can see that the jet head accelerates drastically after entering the hydrogen envelope. In addition, we find that the jet head propagates faster than the cocoon edge all the way through the stellar envelope except for the very early time. We also find that the jet head breaks out of the stellar envelope ~ 400 sec after the central engine is activated. Thus, we conclude that a $40M_{\odot}$ Pop III star has the possibility to raise a GRB.

Note here that $40M_{\odot}$ Pop III stars are thought to end their lives as blue super giants (BSG), keeping large hydrogen envelopes with radii $\sim 10^{12}$ cm. This is because the opacity is too low to induce the mass loss from metal free stellar envelopes (Woosley et al. 2002). In general, the progenitor of a local long GRB is not considered to be a super giant star with a hydrogen or helium envelope but to be a Wolf-Rayet star with no hydrogen or helium envelope and radius $\sim 10^{10}$ cm. The observational reason is that every supernovae associating with long GRBs belongs to type Ibc. Theoretically, it is considered that a super giant star has a too largely extended envelope for the jet to break out successfully (Matzner 2003) and it cannot raise a GRB. From the results here, however, we confirm that a BSG ($\sim 10^{12}$ cm) is compact enough for a successful jet breakout.

We should note that Mészáros & Rees (2001) and Woosley & Heger (2012) have suggested the possibility of GRBs or gamma-ray transients from BSGs. However the former treated a steady jet and did not quantitatively evaluate the possibility, while the latter focused on the formation of the accretion disk around the BH and did not discuss the jet break out. In this section we quantitatively confirm the possibility of GRBs from BSGs by consistently considering the stellar collapse, non-steady jet injection, and the jet propagation.

3. Observational Properties of Pop III GRBs

3.1. The prompt emission

In this section, we consider observational characters of Pop III GRBs. We assume that soon after the jet breakout, the jet emission can be seen as a GRB and the burst lasts until the whole stellar envelope accretes completely. We suppose that the efficiency for converting the jet energy to the radiation energy is 10 %. Accordingly, we can calculate expected properties of the burst, such as the peak luminosity (L_p), duration (T_{90}) and the isotropic energy ($E_{\gamma, \text{iso}}$). Note here that we estimate the T_{90} as the period during which 90 % of the burst’s energy is emitted. Furthermore, we evaluate the time-integrated spectrum using empirical laws for GRBs. There are some correlations which hold between the time-integrated spectral peak energy in the observer frame (E_p^{obs}) and the peak luminosity (L_p)

or the isotropic energy ($E_{\gamma,\text{iso}}$). One is the $E_p - L_p$ correlation (Yonetoku et al. 2004) and the other is the $E_p - E_{\gamma,\text{iso}}$ correlation (Amati et al. 2002). The functional forms of these two correlations are represented as

$$\frac{L_p}{10^{52} \text{ erg sec}^{-1}} \sim 2 \times 10^{-5} \left[\frac{E_p^{\text{obs}}(1+z)}{1 \text{ keV}} \right]^{2.0}, \quad (5)$$

$$\left[\frac{E_p^{\text{obs}}(1+z)}{1 \text{ keV}} \right] \sim 80 \left[\frac{E_{\gamma,\text{iso}}}{10^{52} \text{ erg}} \right]^{0.57}, \quad (6)$$

respectively.

Table 1 shows the results of our model for a $40M_\odot$ Pop III star. As can be seen from Table 1, Pop III GRBs radiate as much energy ($E_{\gamma,\text{iso}} \sim 10^{54} \text{ erg}$) as the most energetic local long GRBs do, while $L_p \sim 5 \times 10^{50} \text{ erg sec}^{-1}$ is smaller by a factor of ~ 10 . Moreover, the duration ($\sim 10^5 \text{ sec}$) of Pop III GRBs is much longer than that of local long GRBs.¹ All these differences come from the fact that although the progenitor of a local long GRB has no hydrogen envelope and is more compact, a Pop III progenitor has a large hydrogen envelope. Since a Pop III star experiences no mass loss and keeps a more massive hydrogen envelope, the energy supply to the central engine can last longer time. This enables the central engine to be kept active for much longer time. This also enables the burst to have a much longer duration and to have the vast isotropic energy. On the other hand, it takes longer time for the jet to break out the larger stellar envelope and the jet energy after the breakout is more damped. This causes the Pop III GRBs to have lower luminosities.

We evaluate the observed peak energy for either the case that the $E_p - L_p$ correlation holds or that the $E_p - E_{\gamma,\text{iso}}$ correlation does. For the case of $E_p - L_p$ correlation, $E_p^{\text{obs}} \sim 5 \text{ keV}$ is in the X-ray region, whereas for the $E_p - E_{\gamma,\text{iso}}$ correlation, the peak energy in the GRB frame is larger than that of a local long GRB, because of the larger $E_{\gamma,\text{iso}}$ value. However, the cosmological redshift effect reduces the peak down to $E_p^{\text{obs}} \sim 120 \text{ keV}$, which is slightly softer than that of a local long GRB.

¹In Suwa & Ioka (2011), they evaluated the duration of the Pop III GRB from a $915M_\odot$ star as $\sim 1,500 \text{ sec}$ in the GRB frame, but this is a wrong value. We find that the correct value is $\sim 15,000 \text{ sec}$ in the GRB frame, which is similar to the one obtained here ($\sim 6000 \text{ sec}$ in the GRB frame). This is because the larger mass of the $915M_\odot$ Pop III star compensates with its larger radius ($\sim 10^{13} \text{ cm}$), as we can see from the expression of the free-fall time.

3.2. The detectability of Pop III GRBs

In this subsection, we discuss the detectability of Pop III GRBs. In Suwa & Ioka (2011), they found that Pop III GRBs are too dim to trigger *Swift* Burst Alert Telescope (BAT). We obtain the similar conclusion even we employ the different progenitor from them. Therefore, we here discuss whether Pop III GRBs trigger the future satellite missions such as *Lobster* (Gehrels et al. 2012) and *EXIST*² in detail. While *Lobster* will have energy window range of 0.3 – 5 keV, *EXIST* will have that of 5 – 600 keV.

An event is regarded to be detected if the number of the signal photons within the detector energy range $[E_{\min}, E_{\max}]$ satisfies the following relation,

$$\frac{\int_{t_0}^{t_0+\Delta t} N_{\text{sig}}(t'_{\text{obs}}) dt'_{\text{obs}} A}{\left(\int_{t_0}^{t_0+\Delta t} N_{\text{bg}} dt'_{\text{obs}} A \right)^{1/2}} \gtrsim (S/N)_{\min}. \quad (7)$$

Here, t_0 is the time when an event comes in the detector’s field of view and the detector starts to observe the event, Δt is the exposure time for the event, and t_{obs} is the time from the beginning of the burst in the observer frame. N_{sig} , A and N_{bg} refer to the signal photon number flux, the area of the detector and the number flux of background photons, respectively. $(S/N)_{\min}$ is the critical signal to noise ratio needed for detection. Assuming that the background photon flux is constant and using the signal photon energy flux within the detector energy window range $[E_{\min}, E_{\max}]$, Eq. (7) can be written as

$$\bar{f}_{\text{sig}}(t_0, \Delta t) \gtrsim f_{\text{sen}}(\Delta t), \quad (8)$$

where

$$\bar{f}_{\text{sig}}(t_0, \Delta t) \equiv \frac{\int_{t_0}^{t_0+\Delta t} f_{\text{sig}}(t'_{\text{obs}}) dt'_{\text{obs}}}{\Delta t} \quad (9)$$

is the energy flux averaged over the exposure time and

$$f_{\text{sen}}(\Delta t) \equiv \frac{\int_{t_0}^{t_0+\Delta t} f_{\text{sig}} dt'_{\text{obs}}}{\int_{t_0}^{t_0+\Delta t} N_{\text{sig}} dt'_{\text{obs}}} (S/N)_{\min} A^{-1/2} N_{\text{bg}}^{1/2} \Delta t^{-1/2} \quad (10)$$

is the energy flux sensitivity within $[E_{\min}, E_{\max}]$. In our model, $f_{\text{sig}}(t_{\text{obs}})$ can be calculated from

$$f_{\text{sig}}(t_{\text{obs}}) = \frac{L_{\gamma, \text{iso}}(t_{\text{obs}})}{4\pi d_L^2} \frac{\int_{E_{\min}}^{E_{\max}} EN(E) dE}{\int_0^\infty EN(E) dE} \text{ erg cm}^{-2} \text{ sec}^{-1}. \quad (11)$$

²<http://exist.gsfc.nasa.gov/>

In Eq. (11), $L_{\gamma,\text{iso}}(t_{\text{obs}})$ is the isotropic equivalent luminosity of the burst at t_{obs} . d_L is the luminosity distance calculated with cosmological parameters $(\Omega_m, \Omega_\Lambda) = (0.28, 0.72)$ and the Hubble parameter $H_0 = 70 \text{ km sec}^{-1} \text{ Mpc}^{-1}$. $N(E)$ is the Band spectrum (Band et al. 1993) with the typical parameter values, $\alpha = -1$ and $\beta = -2.3$. We discuss the detectability of Pop III GRBs for either the case that the $E_p - L_p$ correlation holds or that the $E_p - E_{\gamma,\text{iso}}$ correlation does.

First, we consider the case of the $E_p - L_p$ correlation. Since $E_p^{\text{obs}} \sim 5 \text{ keV}$, in this case *Lobster* is more appropriate for detecting Pop III GRBs. Recently, Ghirlanda et al. (2010) studied the time dependent spectral characteristics of several individual bright GRBs. They found that the isotropic equivalent luminosity $L_{\gamma,\text{iso}}(t_{\text{obs}})$ correlates with the time resolved spectrum peak energy $E_p(t_{\text{obs}})$ for each GRB and that the functional form of the correlation is very similar to the time integrated $E_p - L_p$ correlation (Eq. (5)). Note that they calculated the time resolved spectrum by integrating the signal flux within 1 sec time bin around each time. Accordingly, if we assume the validity of the time-resolved $E_p(t_{\text{obs}}) - L_{\gamma,\text{iso}}(t_{\text{obs}})$ correlation, which is obtained by replacing L_p and E_p^{obs} in Eq. (5) by $L_{\gamma,\text{iso}}(t_{\text{obs}})$ and $E_p^{\text{obs}}(t_{\text{obs}})$, we can discuss the detectability using the condition in Eq. (8).

The *Lobster* sensitivity for a soft source (a power-law photon index of -2) is estimated to be $1.3 \times 10^{-11} \text{ erg cm}^{-2} \text{ sec}^{-1}$ ($0.3 - 5 \text{ keV}$, 5σ) at one calendar day (an effective exposure time of $\sim 2500 \text{ sec}$; see Gehrels et al. 2012). On the other hand, the sensitivity for a proposed exposure time per pointing in a realistic operation ($\sim 450 \text{ sec}$) is calculated to be $3.1 \times 10^{-11} \text{ erg cm}^{-2} \text{ sec}^{-1}$ ($0.3 - 5 \text{ keV}$, 5σ). The assumed spectral parameter in this estimation is reasonable for a GRB with $E_p^{\text{obs}} \sim$ a few keV. We discuss the detectability of a Pop III GRB by *Lobster* using the sensitivity in $\Delta t \sim 450 \text{ sec}$ as a realistic case and in $\Delta t \sim 2500 \text{ sec}$ as an optimistic case.

In Fig. 2, we compare the energy flux of GRBs from $40M_\odot$ Pop III stars with the detection thresholds of *Lobster*. The abscissa is the time from the beginning of a GRB, i.e. from the jet break out, in the observer frame. The green, sky-blue and the blue solid lines represent $f_{\text{sig}}(t_{\text{obs}})$ of Pop III GRBs at $z = 9, 14$ and 19 , respectively, calculated from Eq. (11). The red and magenta dashed lines correspond to f_{sen} of *Lobster* in a realistic case (magenta) and an optimistic case (red). From Fig. 2, we can see that $f_{\text{sig}}(t_{\text{obs}})$ does not change significantly over $\Delta t \sim 450 \text{ sec}$ or $\sim 2500 \text{ sec}$ around each time, so we can approximate $f_{\text{sig}} \sim \text{const.}$ over the considered exposure times. Then, Eq. (8) can be rewritten as

$$f_{\text{sig}}(t_0) \gtrsim f_{\text{sen}}(\Delta t). \quad (12)$$

Eq. (12) indicates that if $f_{\text{sig}}(t_0)$ when an event comes into the *Lobster* field of view is larger than $f_{\text{sen}}(\Delta t)$ for given Δt , we can observe the event from t_0 to $t_0 + \Delta t$. From Fig. 2, we find that Pop III GRBs at $z = 9, 14$ and even at $z = 19$ have the possibility to trigger

Lobster. *Lobster* will detect a Pop III GRB as a long duration X-ray flash with nearly constant luminosity.

Subsequently, we consider the case of the $E_p - E_{\gamma,\text{iso}}$ correlation. Since $E_p^{\text{obs}} \sim 120$ keV, in this case *EXIST* is the better instrument for detection. Note that the $E_p - E_{\gamma,\text{iso}}$ correlation is the correlation between the total radiated energy and the time-integrated spectrum, we can regard E_p^{obs} as the observed peak energy time-averaged within each burst. So, we evaluate $f_{\text{sig}}(5-600 \text{ keV})$ assuming that the spectrum is the Band type with $E_p^{\text{obs}} \sim 120$ keV, $\alpha = -1$ and $\beta = -2.3$ and that the spectrum does not change with time. The sensitivity of *EXIST* for a proposed exposure time in the longest time-scale at the on-board process ($\Delta t \sim 512$ sec) is calculated to be $f_{\text{sen}} \sim 2.4 \times 10^{-10} \text{ erg cm}^{-2} \text{ sec}^{-1}$ (5 – 600 keV, 5σ) (Hong et al. 2009).

We show the results for $40M_{\odot}$ Pop III stars in Fig. 3. Here again, the abscissa is the time from the beginning of a burst, i.e. from the jet break out, in the observer frame. The green, sky-blue and the blue solid lines represent $f_{\text{sig}}(t_{\text{obs}})$ of Pop III GRBs at $z = 9, 14$ and 19 , respectively, calculated from Eq. (11). The red dashed line represents the *EXIST* sensitivity described above. In this case also, $f_{\text{sig}}(t_{\text{obs}})$ is approximately constant over $\Delta t \sim 512$ sec, so Eq. (8) can be rewritten in the form Eq. (12). From Fig. 3, we can see that although Pop III GRBs at $z = 14$ and 19 do not trigger *EXIST*, Pop III GRBs at $z = 9$ have the possibility to trigger *EXIST*. *EXIST* will detect such a Pop III GRB as a long duration X-ray rich GRB with nearly constant luminosity.

3.3. Other progenitor models

McKee & Tan (2008) and Hosokawa et al. (2011) studied the mass of a Pop III star at its birth by calculating the evolution of a primordial protostar in analytical or numerical way. Because the initial angular momentum of a primordial gas cloud is considered to be large enough, in the star formation phase, a protostar and a circumstellar accretion disk system is formed and the protostar gains mass by the accretion of the surrounding gas through the disk. They found that the UV radiation from the protostar eventually stops the mass accretion and the growth of the star by evaporating the surrounding gas and eventually the disk. They also found that the final mass of a Pop III star depends on the degree of the angular momentum transport within the accretion disk and on the magnitude of the initial angular momentum of a gas cloud. In Hosokawa et al. (2011), the degree of the angular momentum transport is characterized by the α_0 -parameter of the disk, where the larger α_0 value means the larger mass accretion. In fig. S1 of Hosokawa et al. (2011), a Pop III star finally gains $\sim 50M_{\odot}$ with $\alpha_0 = 1.0$, $\sim 40M_{\odot}$ with $\alpha_0 = 0.6$ (fiducial case), and $\sim 35M_{\odot}$

with $\alpha_0 = 0.3$, for the fiducial magnitude of the initial angular momentum. Furthermore, the mass of a Pop III star depends on the initial angular momentum of the star-forming gas cloud and it gets $\sim 85M_\odot$ when the initial angular momentum is reduced by 30 % of the fiducial one with $\alpha_0 = 0.6$ (fiducial case).

Accordingly, in this subsection, we investigate whether $30 - 90M_\odot$ Pop III stars can be the progenitors of GRBs. The stellar models of $30 - 40M_\odot$ are given by Woosley et al. (2002) and those of $41 - 90M_\odot$ are from Heger & Woosley (2010). In Fig. 4, we show the density profiles of selected models. Woosley et al. (2002) showed that all the $30 - 40M_\odot$ Pop III stars end their lives as blue super giants (BSG). According to Heger & Woosley (2010), although $41 - 44, 60$ and $70M_\odot$ Pop III stars end as BSGs, $45, 50, 55, 65, 75, 80, 85$ and $90M_\odot$ Pop III stars end as red super giants (RSG). As shown in Heger & Woosley (2010), the RSG branch in the higher mass stars appears due to the primary nitrogen production in the hydrogen burning shell.

For these stellar models, we investigate whether these stars can raise GRBs by considering the jet propagation in the stellar envelope with the entirely similar manner as in §2. Note here that although for a Pop III star with $M \lesssim 40M_\odot$ the fall back effect should be taken into consideration in the formation of a black hole remnant (see e.g., MacFadyen et al. 2001; Kumar et al. 2008), we neglect this effect in this section and discuss it in §4. For BSGs ($30 - 44, 60$ and $70M_\odot$), the jet head propagates faster than the cocoon edge almost all the way through the stellar envelope like in Fig. 1. On the other hand, for RSGs, we find that the jet head reaches the surface as early as or even later than the cocoon edge does. Therefore, we conclude that although Pop III BSGs ($30 - 44, 60, 70M_\odot$) have the possibility to raise GRBs, Pop III RSGs do not. From the above discussions, we can say that although Pop III BSGs ($\sim 10^{12}$ cm) are compact enough for successful jet breakouts, Pop III RSGs ($\sim 10^{14}$ cm) have too largely extended low density envelopes for jets to break out successfully (Fig. 4).

Subsequently, we evaluate the observational characters and the detectability of these Pop III GRBs at $z = 19$. The results for some models are shown in Table 2. We can see the same characteristics for Pop III GRBs as described in §3.1. Here again, we consider either the case that the $E_p - L_p$ correlation holds or that the $E_p - E_{\gamma, \text{iso}}$ correlation holds. First, we consider the case of the $E_p - L_p$ correlation. In Fig. 5, the red and the magenta dashed lines represent $f_{\text{sen}}(\Delta t)$ (0.3-5 keV, 5σ) of *Lobster* in the optimistic and realistic case, respectively (Gehrels et al. 2012). The green, blue, sky-blue, grey and black solid lines correspond to the energy flux $f_{\text{sig}}(t_0)$ of Pop III GRBs at $z = 19$ for $30, 40, 44, 60$ and $70M_\odot$ progenitors, respectively. The abscissa is the time from the beginning of each burst, i.e. from the jet break out. We find that while it is difficult for Pop III GRBs from 60 and $70 M_\odot$ progenitors

to trigger *Lobster*, Pop III GRBs from $\lesssim 44M_{\odot}$ stars have the possibility to trigger *Lobster*. Second, we consider the case of the $E_p - E_{\gamma, \text{iso}}$ correlation and Fig. 6 shows the results. The red dashed line represents the *EXIST* sensitivity. Here also, the green, blue, sky-blue, grey and black solid lines correspond to the energy flux $f_{\text{sig}}(t_0)$ of Pop III GRBs for 30, 40, 44, 60 and $70M_{\odot}$ progenitors, respectively, but at $z = 9$. We find that only Pop III GRBs from $\lesssim 44M_{\odot}$ stars have the possibility to trigger *EXIST*.

From Fig. 5 and Fig. 6, we can see that the energy fluxes of Pop III GRBs from $\lesssim 44M_{\odot}$ progenitors are larger by a factor of 3 to 4 than those from 60, $70M_{\odot}$ stars. This is because more massive progenitors exhibit larger radii (see Fig. 4). The larger radius a progenitor has, the longer time it takes for the jet to reach the stellar surface and the more damped the jet luminosity after the breakout is.

3.4. The afterglow

In this subsection, let us discuss the afterglow of a Pop III GRB following Toma et al. (2011). In the external shock model of an afterglow, we consider that a relativistic ejecta with isotropic equivalent kinetic energy E_{iso} and a half opening angle θ_j moves through the interstellar medium with density n making a shocked region at the head of it. In the shocked region, some fractions, ϵ_B and ϵ_e , of the internal energy are provided to the magnetic field energy and the energy for the electron acceleration, respectively. The accelerated electrons are assumed to have a number distribution of the form $N(\gamma_e) \propto \gamma_e^{-p}$ and to raise afterglow emissions through the synchrotron radiation and the inverse Compton emission. As fiducial parameter values of the external shock model, we adopt $E_{\text{iso}} \sim 10^{55}$ erg, $n = 1 \text{ cm}^{-3}$, $\epsilon_e = 0.1$, $\epsilon_B = 0.01$, $\theta_j = 0.1$ and $p = 2.3$. In §3, we assumed that 10 % of the jet energy was converted into the energy for the prompt photon emission. Accordingly, we consider that the remaining 90 % of the jet energy is used for afterglow emissions. As we saw in §3, $E_{\gamma, \text{iso}} \sim 10^{54}$ erg, so here we adopt $E_{\text{iso}} \sim 10^{55}$ erg as a fiducial value. We refer to Toma et al. (2011) for other parameter values. Under this model, we calculate the afterglow light-curves at 10 GHz, 1 GHz and 100 MHz. We show the results in Fig. 7 in the case of a Pop III GRB at $z = 19$. The red, green and the blue solid lines refer to the light curves at 10 GHz, 1 GHz and 100 MHz, respectively.

Let us discuss the detectability of such Pop III GRB radio afterglow emissions. The Low Frequency Array (LOFAR)³ has frequency coverage from 10 to 250 MHz and the detection threshold of 0.2 mJy (1σ level) at 100 MHz for 1 hr integration time. From Fig. 7, we find

³<http://www.astron.nl/>

that the 100 MHz radio afterglow emission is not detectable by LOFAR. On the other hand, the Expanded Very Large Array (EVLA) has frequency coverage from 1 to 50 GHz and the detection thresholds of $5.5 \mu\text{Jy}$ and $1.8 \mu\text{Jy}$ (1σ level) at 1 GHz and 10 GHz, respectively for 1 hr integration time (Perley et al. 2011). From Fig. 7, we can see that the energy fluxes at 1 GHz and 10 GHz are much larger than the detection thresholds of EVLA. Once a Pop III afterglow emerges, we have the possibility to detect it at any time by EVLA, even if it occurs at such a high redshift universe ($z = 19$).

4. Summary and discussion

GRBs are the brightest phenomena in the universe. Their detections at high z universe ($z \sim 9$) motivate us to expect GRBs to be one of the powerful tools to probe the early universe. Focusing on the high z universe, we should consider the association of GRBs with Pop III stars. Recent numerical simulations (Hosokawa et al. 2011) suggest that Pop III stars obtain mass typically $\sim 40M_{\odot}$ at their birth. Zero metallicity stars are considered not to lose mass during entire life because of the low opacity envelopes (Woosley et al. 2002). Therefore, they enter into the pre-supernova stage keeping large hydrogen envelopes. According to Woosley et al. (2002) and Heger & Woosley (2010), Pop III stars end their lives as BSGs or RSGs depending on the amount of primary nitrogen produced in the shell burning.

In this paper, we investigate whether such low mass Pop III stars ranging from 30 to $90M_{\odot}$ can be progenitors of GRBs. For this purpose, we consider the jet propagation in the stellar envelope and analytically calculate the evolution of the jet-cocoon structure. In BSG envelopes, the jet head velocity is larger than the cocoon velocity all the way except for the very early time and we can expect a successful jet breakout. On the other hand, in RSG envelopes, the cocoon edge reaches the stellar surface as early as or even earlier than the jet head. We confirm that Pop III RSGs have enough largely extended envelopes for jets to be stalled on the way and cannot raise GRBs as shown in Matzner (2003). We also confirm that Pop III BSGs are compact enough for the successful jet breakout and have the possibility to raise GRBs as suggested in Mészáros & Rees (2001) and Woosley & Heger (2012). It should be noted that the BSG models from Woosley and Heger used above ignored the effect of the rotation on the stellar evolution. Ekström et al. (2008) found that when the rotation is included, Pop III stars within our noticed mass range end up as RSGs not BSGs. But Ekström et al. (2008) considered the evolution of a star with an extremely high rotation velocity as one half the critical velocity. Recent cosmological simulations (Stacy et al. 2010 and Clark et al. 2011), however, suggested that Pop III stars are born in binary systems. In

this case, the angular momentum which the star forming gas clump initially has is divided into the spin of each star and the orbital angular momentum so that these stars may rotate less rapidly. Therefore, we think that such rapidly rotating stars they considered are rare and the calculations based on BSG models from Woosley and Heger make sense.

Using our model, we evaluate observational characters of Pop III GRBs. We predict that although Pop III GRBs radiate as much energy as the most energetic local long GRBs, Pop III GRBs are slightly less luminous than local long GRBs due to their much longer burst duration. Assuming that the $E_p - L_p$ (or $E_p - E_{\gamma,\text{iso}}$) correlation holds for Pop III GRBs, we predict that Pop III GRBs have the much softer (or mildly softer) spectra than local long GRBs in the observer frame. Woosley & Heger (2012) predicted that the gamma-ray transients from low metallicity BSGs have duration of 10^{4-5} sec and the luminosity of 10^{48-49} erg sec $^{-1}$, similar to Pop III GRBs considered here. Their transients are fed by the mass accretion of the outer most layers of stars and the accretion rate onto the BH ($\sim 10^{-4} M_\odot$ sec $^{-1}$) is much smaller than that in the Pop III GRB case, which imply typically from $\sim 10^{-3} M_\odot$ sec $^{-1}$ to $\sim 10^{-2} M_\odot$ sec $^{-1}$. Moreover, they simply assumed a central engine model with the roughly estimated conversion efficiency from the mass accretion to the jet energy as ~ 0.1 , while we consider a central engine which is driven by the magnetic process implicitly taking the disk accretion into account with the efficiency of $\eta \sim 6.2 \times 10^{-4}$.⁴ Note that we choose this value so as for Wolf-Rayet stars to reproduce the energetics of local long GRBs. Therefore, although the characters are similar among them, we expect that gamma-ray transients considered in Woosley & Heger (2012) are different events from GRBs considered in this paper.

We also discuss the detectability of Pop III GRBs by future satellite missions such as *Lobster* and *EXIST* in detail. If the $E_p - E_{\gamma,\text{iso}}$ correlation holds, we have the possibility to detect Pop III GRBs at redshifts $z \sim 9$ as long duration X-ray rich GRBs by *EXIST*. On the other hand, if the $E_p - L_p$ correlation holds, we have the possibility to detect Pop III GRBs up to $z \sim 19$ as long duration X-ray flashes by *Lobster*.

We briefly comment the expected observable GRB rate per year by *Lobster* using the results of de Souza et al. (2011). We calculate the observed GRB rate per year $dN_{\text{GRB}}^{\text{obs}}/dz$ as

$$\frac{dN_{\text{GRB}}^{\text{obs}}}{dz} = \frac{\Omega_{\text{obs}}}{4\pi} \eta_{\text{beam}} \frac{dN_{\text{GRB}}}{dz}, \quad (13)$$

where dN_{GRB}/dz , Ω_{obs} and η_{beam} correspond to the intrinsic GRB rate (the number of on-axis and off-axis GRBs) per year, the detector field of view and the beaming factor of the burst.

⁴Note that Woosley & Heger (2012) considered the rotationally supported disk structure and the mass accretion from it so that the meaning of the conversion efficiency is different from ours.

In Fig. 6 of de Souza et al. (2011), they showed dN_{GRB}/dz for an *optimistic* case and we use their values. Here, we also adopt the values of $\eta_{\text{beam}} \sim 0.01$ and $\Omega_{\text{obs}} \sim 0.5$ sr for *Lobster* (Gehrels et al. 2012). Optimistically speaking, we predict that *Lobster* detects about 40, 4 and 0.4 Pop III GRBs per year at $z = 9, 14$ and 19 , respectively.

At last, we briefly discuss employed assumptions in this paper. Firstly, we assume that all the stars considered in this paper ($30 - 90M_{\odot}$ Pop III stars) form black holes directly after the stellar core collapse (see §3.3). It should be noted, however, that this is not always the case especially for less massive stars. Shortly after the onset of the core collapse, a neutron star and a shock wave, which propagates outward or is stalled, are considered to be formed at first. Behind the shock wave, a fall back accretion of the shocked envelope could be present and the continuous accretion onto the neutron star eventually leads to a black hole formation. Although the early activity of the central engine could be affected by the accretion details, i.e., the direct accretion or fall-back accretion, the conclusion of this paper is hardly changed. This is because the mass accretion at the interested time in this paper is coming from the massive envelope so that the central engine already collapsed to a black hole at the corresponding time. In addition, since the energy budget of the shock head is dominated by the envelope accretion, the details of the early phase does not affect the shock evolution in the late phase. For a more massive ($\gtrsim 40M_{\odot}$) star, on the other hand, the energy of the shock wave is too low to explode even the portion of the envelope, so a black hole would be formed directly and our assumption is fully justified in this case. Note that the mass threshold between the direct or fall-back induced black hole formation is still under the debate (see e.g. Fryer 1999) and beyond the scope of this paper. Secondly, we assume that the whole stellar envelope accretes onto the BH (see §3.1). In order to confirm the validity of this assumption, we evaluate the binding energy of each layer of the stellar envelope and compare it with the typical energy of a supernova outgoing shock $\sim 10^{51}$ erg, which is injected around ~ 10 km from the center. We find that the binding energy becomes larger than 10^{51} erg within $r \lesssim 5 \times 10^9$ cm. This means that the outgoing shock should stall on the way and we expect little mass ejection. Recently, Quataert & Shiode (2012) suggested that in the late stage of the stellar evolution, the pre-supernova burning leads to a significant mass ejection from the outer envelope. But they considered only the case of a $40M_{\odot}$ star with metallicity $Z = 10^{-4}$ and commented that the amount of mass ejection depends on the metallicity and rotation etc. Thus, the amount of the ejectable mass is uncertain for the progenitors employed here so that we do not consider this effect in this paper.

Acknowledgements

We thank A. Heger for kindly providing us his stellar model data. We thank D. Yonetoku and R. Yamazaki for fruitful discussion and suggestions about GRB observations. We also thank K. Omukai for fruitful discussions about Population III stars and the anonymous referee for fruitful comments. This work is supported in part by the Grant-in-Aid from the Ministry of Education, Culture, Sports, Science and Technology (MEXT) of Japan, No.23540305 (TN), No.24103006 (TN), No.23840023(YS) and by the Grant-in-Aid for the global COE program *The Next Generation of Physics, Spun from Universality and Emergence* at Kyoto University.

REFERENCES

- Abel, T., Bryan, G. L., & Norman, M. L. 2002, *Science*, 295, 93
- Amati, L., Frontera, F., Tavani, M., et al. 2002, *A&A*, 390, 81
- Band, D., Matteson, J., Ford, L., et al. 1993, *ApJ*, 413, 281
- Bromm, V., Coppi, P. S., & Larson, R. B. 2002, *ApJ*, 564, 23
- Chandra, P., Frail, D. A., Fox, D., et al. 2010, *ApJ*, 712, L31
- Chitre, D. M., & Hartle, J. B. 1976, *ApJ*, 207, 592
- Clark, P. C., Glover, S. C. O., Klessen, R. S., & Bromm, V. 2011, *ApJ*, 727, 110
- Cucchiara, A., Levan, A. J., Fox, D. B., et al. 2011, *ApJ*, 736, 7
- de Souza, R. S., Yoshida, N., & Ioka, K. 2011, *A&A*, 533, A32
- Ekström, S., Meynet, G., Chiappini, C., Hirschi, R., & Maeder, A. 2008, *A&A*, 489, 685
- Fryer, C. L. 1999, *ApJ*, 522, 413
- Fryer, C. L., Woosley, S. E., & Heger, A. 2001, *ApJ*, 550, 372
- Gehrels, N., Barthelmy, S. D., & Cannizzo, J. K. 2012, *IAU Symposium*, 285, 41
- Ghirlanda, G., Nava, L., & Ghisellini, G. 2010, *A&A*, 511, A43
- Grindlay, J., & EXIST Team 2009, *American Institute of Physics Conference Series*, 1133,

- Heger, A., Fryer, C. L., Woosley, S. E., Langer, N., & Hartmann, D. H. 2003, *ApJ*, 591, 288
- Heger, A., & Woosley, S. E. 2010, *ApJ*, 724, 341
- Hjorth, J., & Bloom, J. S. 2011, arXiv:1104.2274
- Hong, J., Grindlay, J. E., Allen, B., et al. 2009, *Proc. SPIE*, 7435,
- Hosokawa, T., Omukai, K., Yoshida, N., & Yorke, H. W. 2011, *Science*, 334, 1250
- Komissarov, S. S., & Barkov, M. V. 2010, *MNRAS*, 402, L25
- Kumar, P., Narayan, R., & Johnson, J. L. 2008, *MNRAS*, 388, 1729
- MacFadyen, A. I., & Woosley, S. E. 1999, *ApJ*, 524, 262
- MacFadyen, A. I., Woosley, S. E., & Heger, A. 2001, *ApJ*, 550, 410
- Matzner, C. D. 2003, *MNRAS*, 345, 575
- McKee, C. F., & Tan, J. C. 2008, *ApJ*, 681, 771
- Mészáros, P., & Rees, M. J. 2001, *ApJ*, 556, L37
- Mészáros, P., & Rees, M. J. 2010, *ApJ*, 715, 967
- Nagakura, H., Suwa, Y., & Ioka, K. 2012, *ApJ*, 754, 85
- Perley, R. A., Chandler, C. J., Butler, B. J., & Wrobel, J. M. 2011, *ApJ*, 739, L1
- Quataert, E., & Shiode, J. 2012, *MNRAS*, 423, L92
- Rhoades, C. E., & Ruffini, R. 1974, *Physical Review Letters*, 32, 324
- Salvaterra, R., Della Valle, M., Campana, S., et al. 2009, *Nature*, 461, 1258
- Stacy, A., Greif, T. H., & Bromm, V. 2010, *MNRAS*, 403, 45
- Suwa, Y., Takiwaki, T., Kotake, K., & Sato, K. 2007, *PASJ*, 59, 771
- Suwa, Y., & Ioka, K. 2011, *ApJ*, 726, 107
- Tan, J. C., & McKee, C. F. 2004, *ApJ*, 603, 383
- Tanvir, N. R., Fox, D. B., Levan, A. J., et al. 2009, *Nature*, 461, 1254
- Toma, K., Sakamoto, T., & Mészáros, P. 2011, *ApJ*, 731, 127

- Turk, M. J., Abel, T., & O’Shea, B. 2009, *Science*, 325, 601
- Yonetoku, D., Murakami, T., Nakamura, T., et al. 2004, *ApJ*, 609, 935
- Woosley, S. E. 1993, *ApJ*, 405, 273
- Woosley, S. E., Heger, A., & Weaver, T. A. 2002, *Reviews of Modern Physics*, 74, 1015
- Woosley, S. E., & Heger, A. 2012, *ApJ*, 752, 32

Table 1: The comparison of typical long GRBs and Pop III GRBs with $40M_{\odot}$.

	long GRB	Pop III GRB ($z = 9$)
$E_{\gamma,\text{iso}}$ [erg]	10^{52-54}	10^{54}
L_p [erg sec $^{-1}$]	10^{52-53}	6×10^{50}
T_{90} [sec]	10^{1-3}	6×10^4
E_p^{obs} [keV]	10^{2-3}	$5.5 (E_p - L_p)$ $120 (E_p - E_{\gamma,\text{iso}})$

Table 2: The observational characteristics of Pop III GRBs at $z = 19$ for various progenitor masses.

mass [M_{\odot}]	30	44	60	70
$E_{\gamma,\text{iso}}$ (10^{54}) [erg]	0.94	1.1	1.5	1.6
L_p (10^{50}) [erg sec $^{-1}$]	5.1	6.4	1.7	1.9
T_{90} (10^5) [sec]	0.87	1.3	10	11
E_p^{obs} [keV] ($E_p - L_p$)	2.5	2.8	1.4	1.5
E_p^{obs} [keV] ($E_p - E_{\gamma,\text{iso}}$)	54	60	70	75

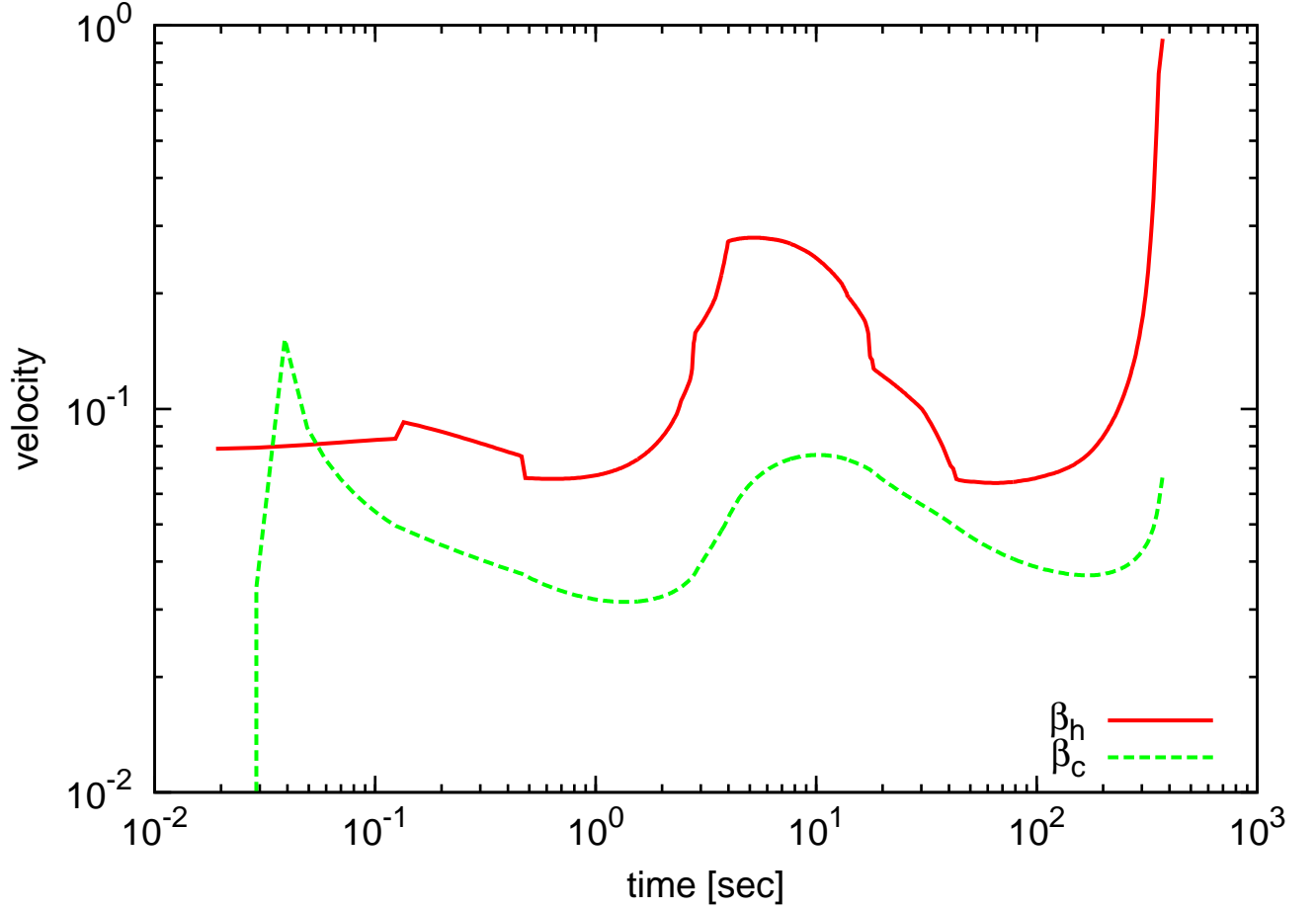


Fig. 1.— The time evolution of the jet head velocity β_h (the red solid line) and the cocoon velocity β_c (the green dashed line) during the propagation in the stellar envelope. The abscissa is the time from which the jet is activated. The progenitor is a $40M_\odot$ Pop III star.

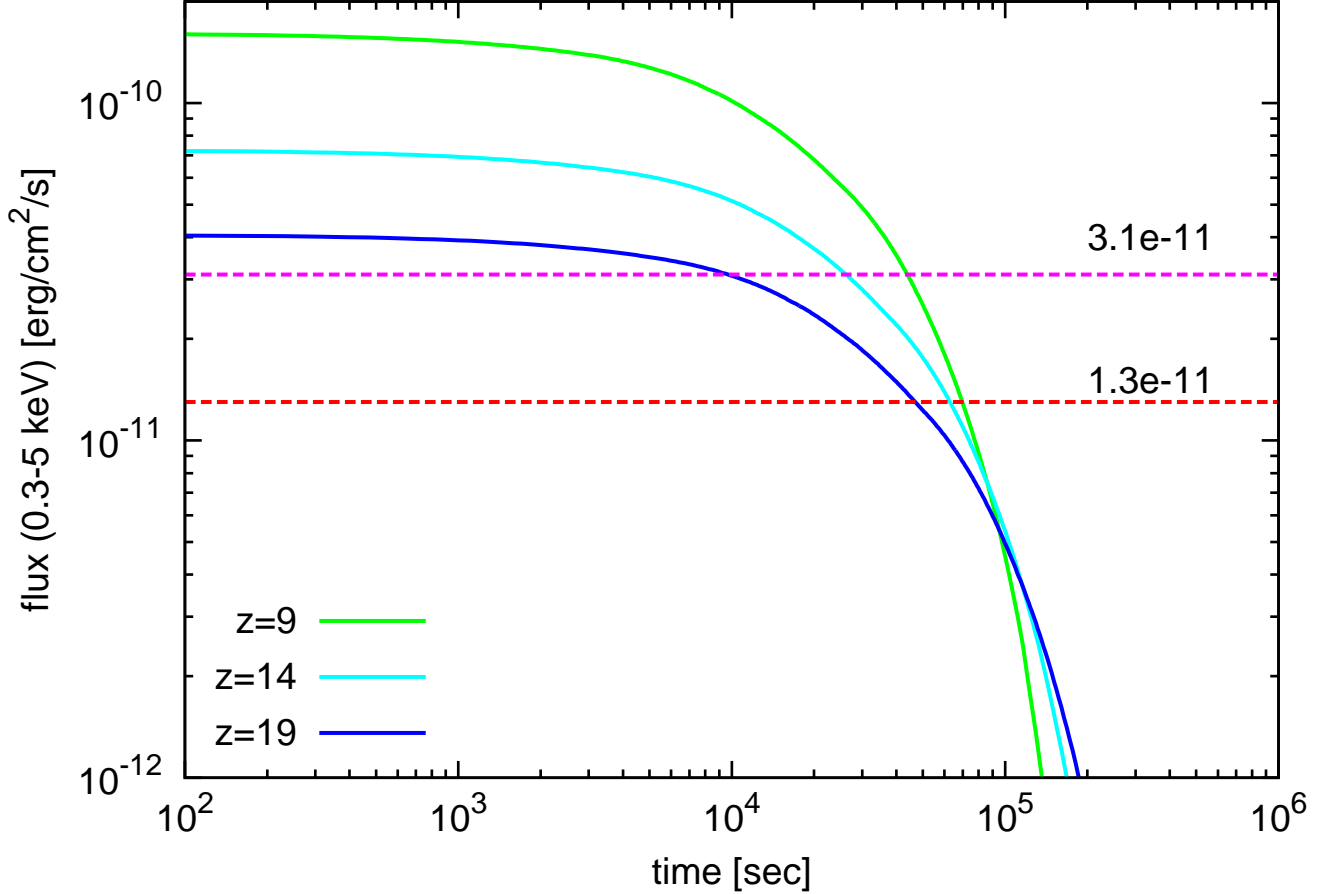


Fig. 2.— The comparison of the energy flux $f_{\text{sig}}(t_0)$ for a Pop III GRB with the detection thresholds of *Lobster*, $f_{\text{sen}}(\Delta t)$ (0.3-5 keV, 5σ). The abscissa is the time from the beginning of a GRB, i.e., from the jet break out, in the observer frame. t_0 is the time when the event comes into the *Lobster* field of view and *Lobster* starts to observe the event. Δt is the proposed exposure time of *Lobster*. The green, sky-blue and the blue solid lines correspond to f_{sig} (0.3-5 keV) for the GRB from a $40M_{\odot}$ Pop III star at $z = 9, 14$ and 19 , respectively. The red and the magenta dashed lines represent $f_{\text{sen}}(\Delta t)$ (0.3-5 keV, 5σ) of *Lobster* (Gehrels et al. 2012), corresponding to the optimistic case of $\Delta t \sim 2500$ sec and the realistic case of $\Delta t \sim 450$ sec, respectively. If $f_{\text{sig}}(t_0) \gtrsim f_{\text{sen}}(\Delta t)$ holds, we regard that *Lobster* observes the Pop III GRB from t_0 to $t_0 + \Delta t$.

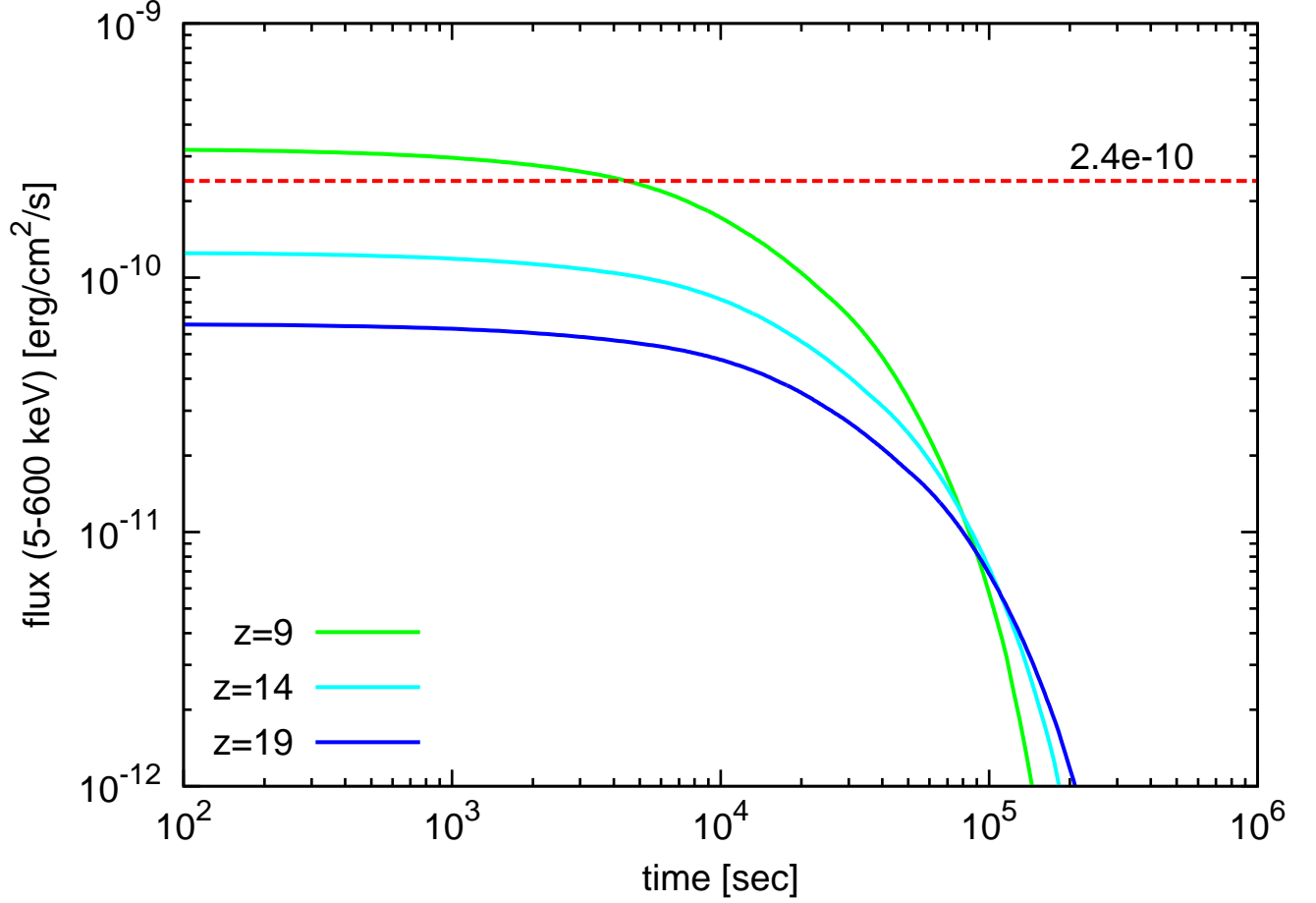


Fig. 3.— Same as Fig. 2 but for *EXIST* case. *EXIST* will have the limited energy range of 5-600 keV. The red dashed line represents the *EXIST* sensitivity $f_{\text{sen}} \sim 2.4 \times 10^{-10} \text{ erg cm}^{-2} \text{ sec}^{-1}$ (5-600 keV, 5σ) in the longest exposure time-scale at the on-board process ($\Delta t \sim 512 \text{ sec}$) (Hong et al. 2009).

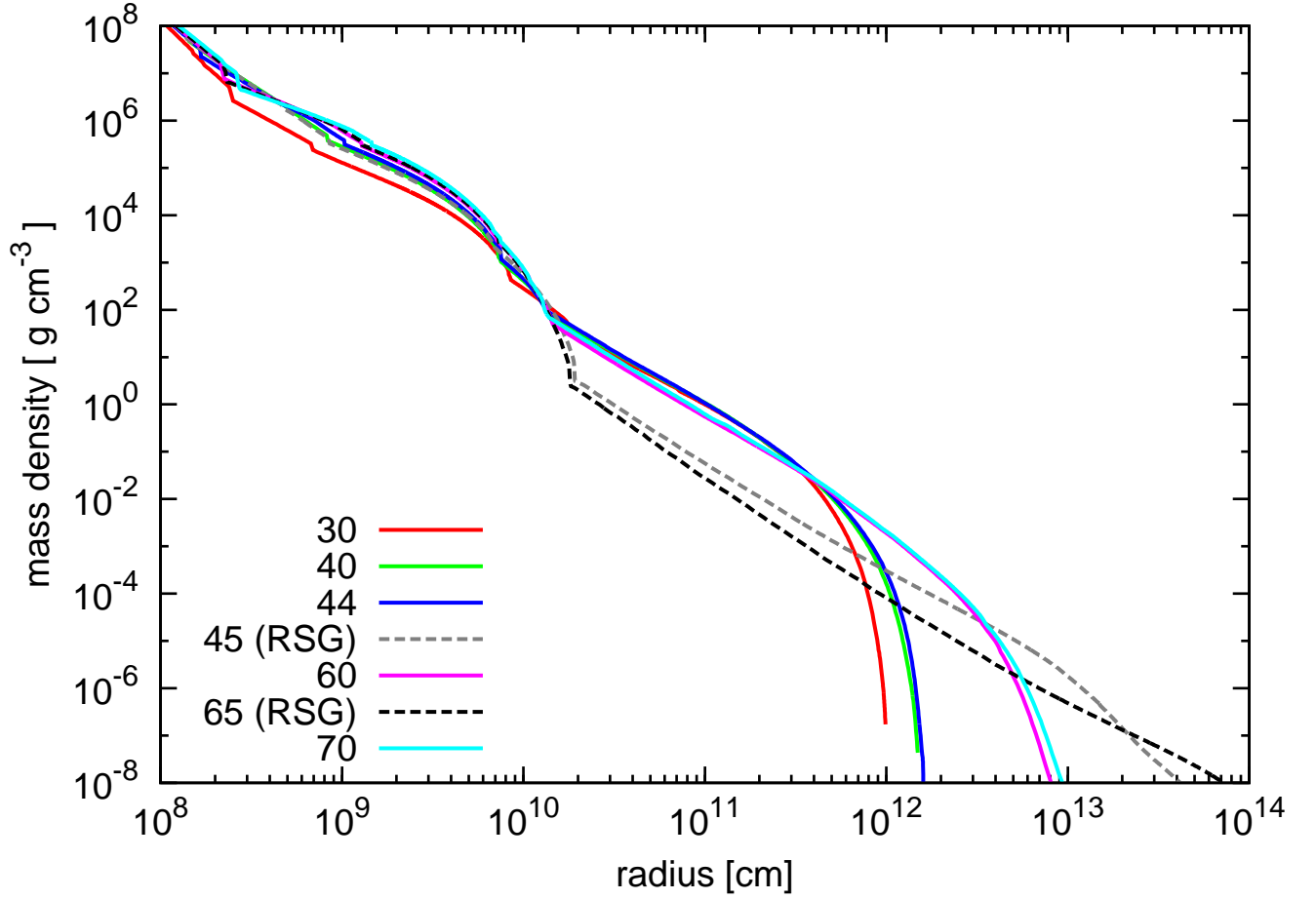


Fig. 4.— The density profiles for some of the Pop III stellar models (Woosley et al. 2002; Heger & Woosley 2010). Those who end their life as BSGs correspond to $30M_{\odot}$ (red), $40M_{\odot}$ (green), $44M_{\odot}$ (blue), $60M_{\odot}$ (magenta) and $70M_{\odot}$ (sky-blue), respectively. They have radii 10^{12-13} cm. Those who end their life as RSGs correspond to $45M_{\odot}$ (grey) and $65M_{\odot}$ (black), respectively. They have radii $\sim 10^{14}$ cm. We can see that RSGs have much more extended and lower density envelopes than BSGs have.

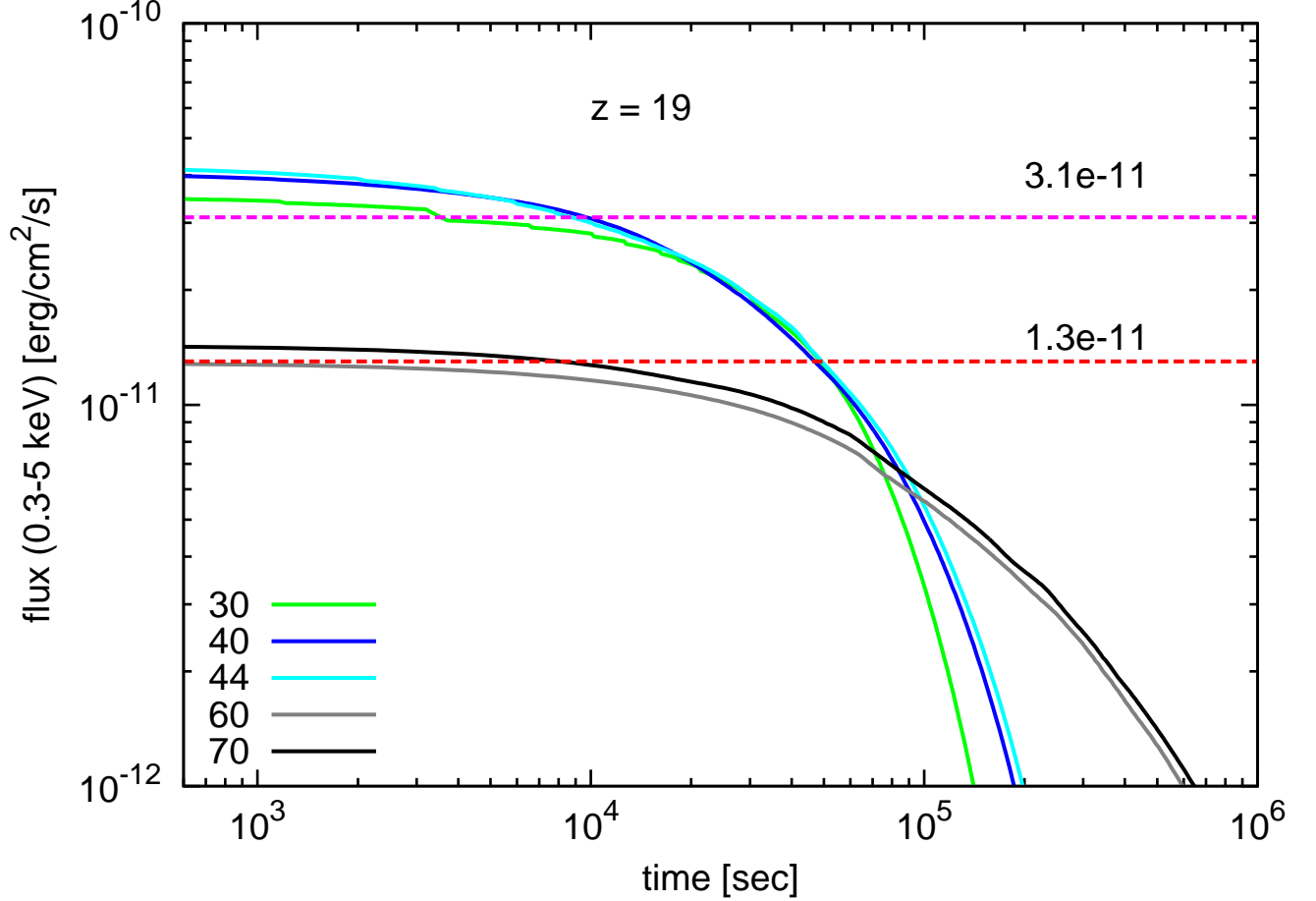


Fig. 5.— The comparison of the energy flux $f_{\text{sig}}(t_0)$ for Pop III GRBs with the detection thresholds of *Lobster*, $f_{\text{sen}}(\Delta t)$ (0.3-5 keV, 5σ). The abscissa is the time from the beginning of a GRB, i.e., from the jet break out, in the observer frame. t_0 is the time when the event comes into the *Lobster* field of view and *Lobster* starts to observe the event. Δt is the proposed exposure time. The green, blue, sky-blue, grey and black solid lines correspond to f_{sig} (0.3-5 keV) of Pop III GRBs at $z = 19$ from 30, 40, 44, 60 and $70M_{\odot}$ progenitors, respectively. The red and the magenta dashed lines represent $f_{\text{sen}}(\Delta t)$ (0.3-5 keV, 5σ) of *Lobster* (Gehrels et al. 2012), corresponding to the optimistic case of $\Delta t \sim 2500$ sec and the realistic case of $\Delta t \sim 450$ sec, respectively. If $f_{\text{sig}}(t_0) \gtrsim f_{\text{sen}}(\Delta t)$ holds, we regard that *Lobster* observes the Pop III GRB from t_0 to $t_0 + \Delta t$.

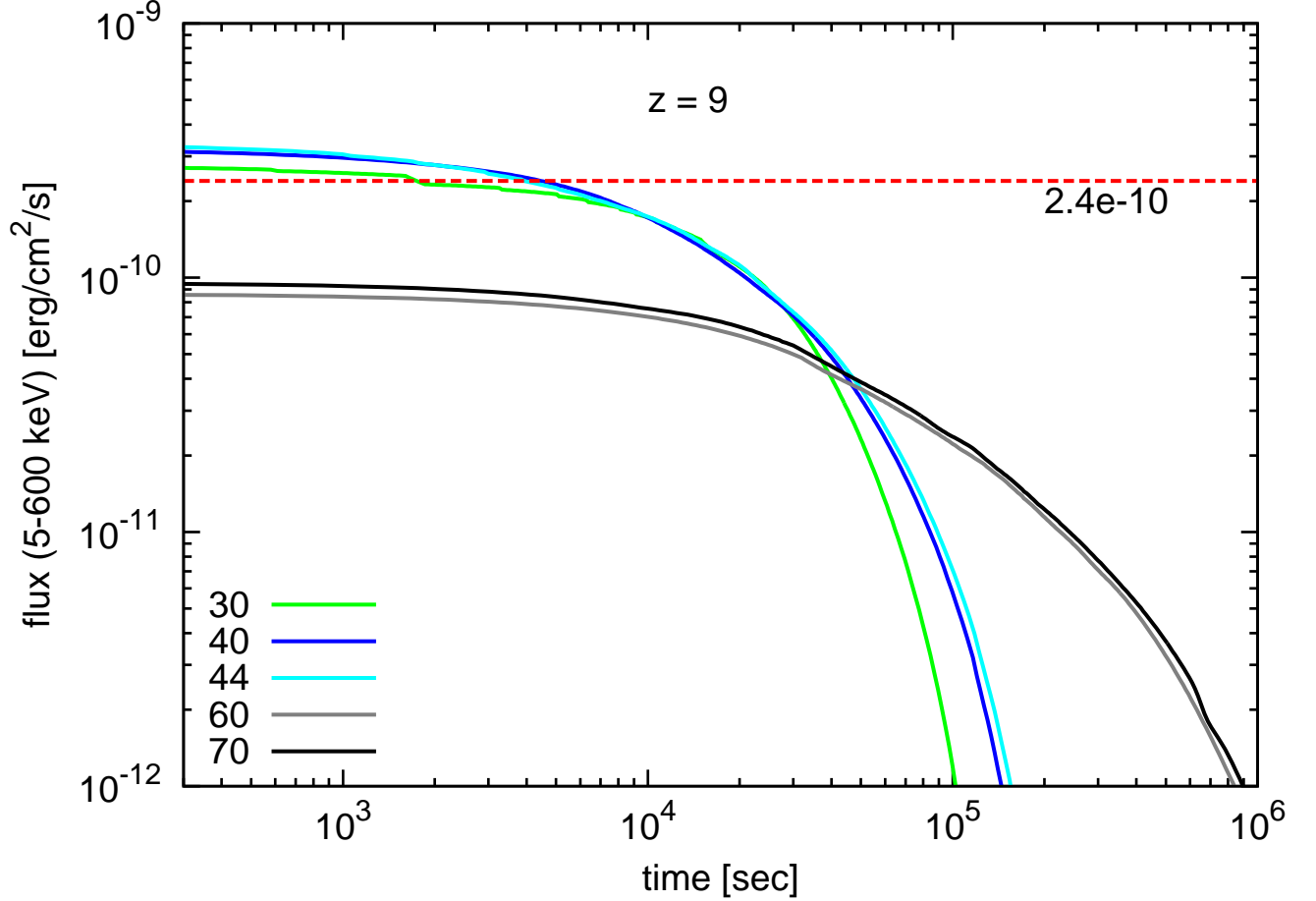


Fig. 6.— Same as Fig. 5, but for *EXIST* (5-600 keV) case. The red dashed line represents the *EXIST* sensitivity $f_{\text{sen}} \sim 2.4 \times 10^{-10} \text{ erg cm}^{-2} \text{ sec}^{-1}$ (5-600 keV, 5σ) in the longest exposure time-scale at the on-board process ($\Delta t \sim 512 \text{ sec}$) (Hong et al. 2009). Note that we focus on Pop III GRBs at $z = 9$ in this figure.

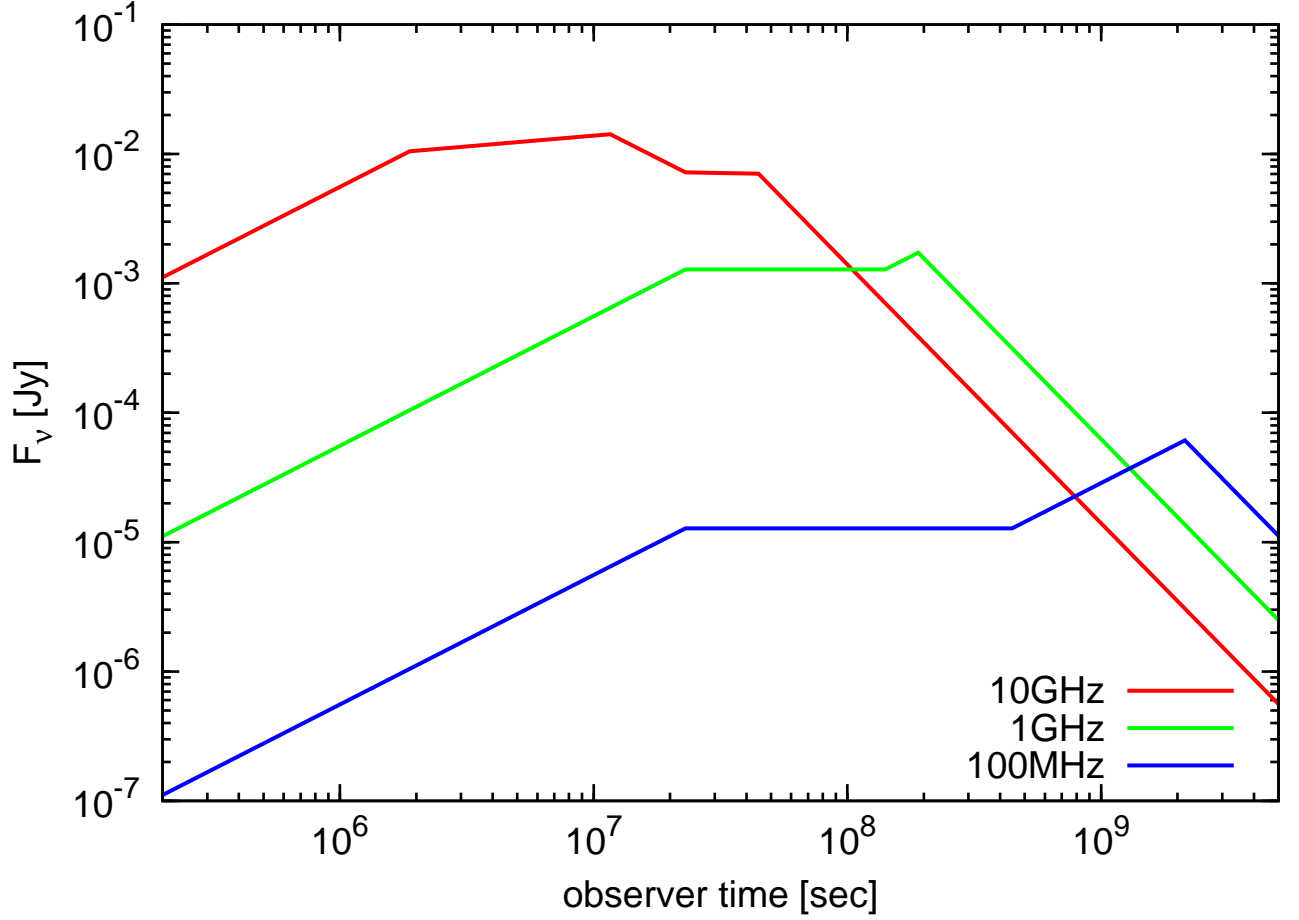


Fig. 7.— The afterglow light-curves of a Pop III GRB at 100 MHz, 1 GHz and 10 GHz in the case that the GRB happens at $z = 19$. The red, green and the blue solid lines correspond to the light-curves at 10 GHz, 1 GHz and 100 MHz, respectively. The abscissa is the time from the beginning of the prompt emission, i.e. from the jet break out time, in the observer frame. Here, we adopt the parameter values of $n = E_{55} = \epsilon_{e,-1} = \epsilon_{B,-2} = f(p) = \theta_{j,-1} = 1$ and $p = 2.3$. Q_x denotes $Q/10^x$.